birds will forage independently soon after leaving the nest. Some pelecaniform birds will begin breeding as soon as the second year (e.g., cormorants), although three years of age seems to be the norm, while in other species (e.g., Abbott's booby) many years may pass before individuals breed.

Status and Conservation

Few of the Pelecaniformes are globally threatened, although some island and inland populations of pelecaniform birds have become extinct in the face of habitat loss and contamination. In some species (e.g., double-crested cormorant, white pelican), numbers are increasing with near-exponential growth, while in others (e.g., Dalmatian pelican) population abundance is rapidly decreasing. Island species and populations have been especially hard-hit by the introduction of terrestrial predators such as cats, rats, and pigs; loss of traditional breeding habitat has played a greater role in aquatic and inland-nesting species. Some islands such as Christmas Island (Indian Ocean) and Ascension Island (Atlantic Ocean) are breeding grounds for several pelecaniform species, and their recent protected status has promised a much better future than might have been possible only a few years earlier.

See also

Seabird Conservation. Seabird Overview. Seabirds as Indicators of Ocean Pollution.

Further Reading

Ashmole NP (1971) Sea bird ecology and the marine environment. In: Farner DS, King JR and Parkes KC (eds) *Avian Biology*, Vol. 1. New York: Academic Press.

Cairns DK (1986) Plumage colour in pursuit diving seabirds: why do penguins wear tuxedos? *Bird Behaviour* 6: 58–65.

Diamond AW (1975) The biology of tropicbirds at Aldabra Atoll, Indian Ocean. *Auk* 92: 16–39.

Frederick PC and Siegel-Causey D (2000) Anhinga (*Anhinga anhinga*). In: Poole A and Gill F (eds) *The Birds of North America*, *No. 522*. Philadelphia, PA: The Birds of North America, Inc.

Johnsgard PA (1993) *Cormorants, Darters, and Pelicans of the World*. Washington, DC: Smithsonian Institution Press.

Nelson JB (1978) *The Sulidae: Gannets and Boobies*. Aberdeen, Oxford University Press.

Nelson JB (1985) Frigatebirds, aggression, and the colonial habit. *Noticias Galapagos* 41: 16–19.

Siegel-Causey D (1986) Behaviour and affinities of the Magellanic Cormorant. *Notornis* **33**: 249–257.

Siegel-Causey D (1988) Phylogeny of the Phalacrocoracidae. *Condor* 90: 885–905.

Siegel-Causey D (1996) The problem of the Pelecaniformes: molecular systematics of a privative group. In: Mindell DL (ed.) *Avian Molecular Evolution and Systematics*. New York: Academic Press.

Van Eerden MR and Voslamber B (1995) Mass fishing by cormorants *Phalacrocorax carbo sinensis* at Lake Ijsselmeer, The Netherlands: a recent successful adaptation to a turbid environment. *Ardea* 83: 199–212.

Van Tets GF (1965) A comparative study of some social communication patterns in the Pelecaniformes. *Ornithological Monographs, No. 2*. Washington, DC: American Ornithological Union.

PELICANS

See **PELICANIFORMES**

PENETRATING SHORTWAVE RADIATION

C. A. Paulson and W. S. Pegau, Oregon State University, Corvallis, OR, USA

doi:10.1006/rwos.2001.0154

Introduction

The penetration of solar radiation into the upper ocean has important consequences for physical, chemical, and biological processes. The principal physical process is the heating of the upper layers by the absorption of solar radiation. To estimate the solar radiative heating rate, the net downward shortwave irradiance entering the ocean and the rate of absorption of this energy as a function of depth must be determined. Shortwave irradiance is the flux of solar energy incident on a plane surface ($W\,m^{-2}$).

Given the downward shortwave radiance field just above the sea surface, the rate of shortwave absorption as a function of depth is governed primarily by sea surface roughness, molecular structure of pure sea water, suspended particles, and dissolved organic compounds. The optical properties of pure sea water are considered a baseline; the addition of particles and dissolved compounds increases absorption and scattering of sunlight. The dissolved organic compounds are referred to as 'colored dissolved organic matter' (CDOM) or 'yellow matter' because they color the water yellowish-brown. The source of CDOM is decaying plants; concentrations are highest in coastal waters. Suspended particles may be of biological or geological origin. Biological (organic) particles are formed as the result of the growth of bacteria, phytoplankton, and zooplankton. The source of geological (inorganic) particles is primarily weathering of terrestrial soils and rocks that are carried to the ocean by the wind and rivers. Phytoplankton particles are the main determinant of optical properties in much of the ocean and the concentration of chlorophyll associated with these plants is used to quantify the effect of phytoplankton on optical properties. Case 1 waters are defined as waters in which the concentration of phytoplankton is high compared with inorganic particles and dissolved compounds; roughly 98% of the world ocean falls into this category. Case 2 waters are waters in which inorganic particles or CDOM are the dominant influence on optical properties. Case 2 waters are usually coastal, but not all coastal water is case 2.

Inherent optical properties (IOPs), such as attenuation of a monochromatic beam of light, depend only on the medium, i.e. IOPs are independent of the ambient light field. It is often assumed that the inherent optical properties of the upper ocean are independent of depth. To the extent that the upper ocean is well-mixed, the assumption of homogeneous optical properties is reasonable. However, in the stratified layers below the mixed layer, the concentration of particles is likely to vary with depth. The consequences of this variation on radiant heating are expected to be small because the magnitude of the downward irradiance decreases rapidly with depth.

Apparent optical properties (AOPs) depend both on the medium and on the directional properties of the ambient light field. Some AOPs, such as the ratio of downward irradiance in the ocean to the surface value, are sufficiently independent of directional properties of the light field to be useful for characterizing the optical properties of a water body.

Albedo

Albedo, A, is the ratio of upward to downward short-wave irradiance just above the sea surface and is defined by:

$$A \equiv \frac{E_u}{E_d}$$

where E_u and E_d are the upwelling and downward irradiances just above the sea surface, respectively. The upwelling irradiance is composed of two components: emergent irradiance due to back-scattered light from below the sea surface; and irradiance reflected from the sea surface. Emergent irradiance is typically $< 10\%$ of reflected irradiance. The rate at which net short-wave irradiance penetrates the sea surface is the rate at which the sea absorbs solar energy and is given by:

$$(1 - A)\, E_d \ (\mathrm{W\,m^{-2}})$$

R.E. Payne analyzed observations to represent albedo as a function of solar altitude θ and atmospheric transmittance Γ defined by:

$$\Gamma = E_d r^2 / S \sin\theta$$

where S is the solar constant ($1370\,\mathrm{W^{-2}}$) and r is the ratio of the actual to mean Earth–sun separation. The transmittance is a measure of the effect of the Earth's atmosphere, including clouds, on the radiance distribution at the Earth's surface. If there were no atmosphere, the transmittance would equal one and the radiance would be a direct beam from the sun. For very heavy overcast, the transmittance can be < 0.1 and the downward radiance distribution may be approximately independent of direction.

Payne's observations were taken from a fixed platform off the coast of Massachusetts from 25 May to 28 September. Solar altitude ranged up to 72° and the mean wind speed was $3.7\,\mathrm{m\,s^{-1}}$. The transmittance varied from near zero to about 0.75. Payne fitted smooth curves to the albedo as a function of transmittance for observations in intervals of 2° of solar altitude and 0.1 in transmittance. The smoothed albedos ranged from 0.03 to 0.5. Payne extrapolated the curves to values of solar altitude and transmittance for which there were no observations by use of theoretical calculations of reflectance for a sea surface roughened by a wind speed of $3.7\,\mathrm{m\,s^{-1}}$. Albedo was obtained for the limiting case of $\Gamma = 1$ by adding 0.005 to the calculated reflectance to account for the irradiance emerging from beneath the surface.

Wind speed affects albedo through its influence on the surface roughness. The clear-sky reflectivity from a flat water surface is a strong function of solar altitude for altitudes $< 30^\circ$. As wind speed and roughness increase, reflectivity decreases because of the nonlinear relationship between reflectivity and the incidence angle. Payne investigated the variation of albedo with wind speed for solar elevations from 17° to 25° and found that albedo decreased at the rate of 2% per meter per second increase in wind speed.

Wind speed may also affect albedo by the generation of breaking waves that produce white caps. The albedo of whitecaps is higher, on average, than the whitecap-free sea surface. Hence the qualitative effect of whitecaps is to increase the albedo. Monahan and O'Muircheartaigh estimate an increase of 10% in albedo due to whitecaps for a wind speed of $15\,m\,s^{-1}$ and of 20% for a wind speed of $20\,m\,s^{-1}$.

Payne estimated monthly climatological values of albedo at 10° latitude intervals for the Atlantic Ocean (**Table 1**). For the range of latitudes from 40°S to 40°N, mean albedo varies from a minimum of 0.06 at the equator in all months to a maximum of 0.11 at 40°S and 40°N for the months containing the winter solstice. The symmetry exhibited by mean albedo values for the winter solstice in the North and South Atlantic suggests that the values in **Table 1** may be reasonable estimates for the world ocean.

Spectrum of Downward Irradiance

The spectrum of downward short-wave irradiance at various depths in the ocean (**Figure 1**) illustrates the strong dependence of absorption on wavelength. The shape of the spectrum at the surface is determined primarily by the temperature of the sun (Wien displacement law) and wavelength-dependent absorption by the atmosphere. The area under the spectrum at each depth is proportional to the downward irradiance. The downward irradiance at a depth of 1 m is less than half the surface value because of preferential absorption at wavelengths in excess of 700 nm. The downward irradiance below 10 m depth is in a relatively narrow band centered near 470 nm (blue-green). Pure sea water is most transparent near a wavelength of 450 nm which, by coincidence, is close to the peak in the downward irradiance spectrum at the surface.

Modeled Irradiance

Radiative transfer models are useful tools for investigating the characteristics of underwater light fields and their dependence on suspended particles and dissolved organic matter. The Hydrolight model, constructed by Mobley, is used to illustrate the diffuse attenuation coefficient for downward irradiance for three cases with different concentrations of chlorophyll and values of CDOM beam attenuation at 440 nm (**Figure 2**). The diffuse attenuation coefficient for downward irradiance K_d is defined by

$$K_d(z, \lambda) = \frac{d \ln E_d(z, \lambda)}{dz}$$

where z is the vertical space coordinate, zero at the surface and positive upward, and λ is the

Table 1 Mean albedos for the Atlantic Ocean by month and latitude

Latitude	*Jan*	*Feb*	*Mar*	*Apr*	*May*	*Jun*	*Jul*	*Aug*	*Sep*	*Oct*	*Nov*	*Dec*
80°N			0.33	0.14	0.10	0.09	0.08	0.08	0.12			
70°N		0.41	0.15	0.10	0.08	0.07	0.07	0.09	0.11	0.25		
60°N	0.28	0.12	0.09	0.07	0.07	0.07	0.06	0.07	0.07	0.10	0.16	0.44
50°N	0.11	0.10	0.08	0.07	0.06	0.06	0.06	0.07	0.07	0.08	0.11	0.12
40°N	0.10	0.09	0.07	0.07	0.06	0.06	0.06	0.06	0.07	0.08	0.10	0.11
30°N	0.09	0.07	0.06	0.06	0.06	0.06	0.06	0.06	0.06	0.07	0.08	0.09
20°N	0.07	0.06	0.06	0.06	0.06	0.06	0.06	0.06	0.06	0.06	0.07	0.07
10°N	0.07	0.06	0.06	0.06	0.06	0.06	0.06	0.06	0.06	0.06	0.06	0.07
0°	0.06	0.06	0.06	0.06	0.06	0.06	0.06	0.06	0.06	0.06	0.06	0.06
10°S	0.06	0.06	0.06	0.06	0.07	0.07	0.06	0.06	0.06	0.06	0.06	0.06
20°S	0.06	0.06	0.06	0.06	0.07	0.07	0.07	0.07	0.06	0.06	0.06	0.06
30°S	0.06	0.06	0.06	0.07	0.08	0.09	0.08	0.07	0.07	0.06	0.06	0.06
40°S	0.06	0.06	0.07	0.08	0.09	0.11	0.10	0.08	0.07	0.07	0.06	0.06
50°S	0.06	0.07	0.07	0.08	0.10	0.13	0.11	0.08	0.08	0.07	0.06	0.06
60°S	0.06	0.07	0.08	0.11	0.13		0.27	0.07	0.08	0.07	0.06	0.06

(Reproduced with permission from Payne, 1972.)

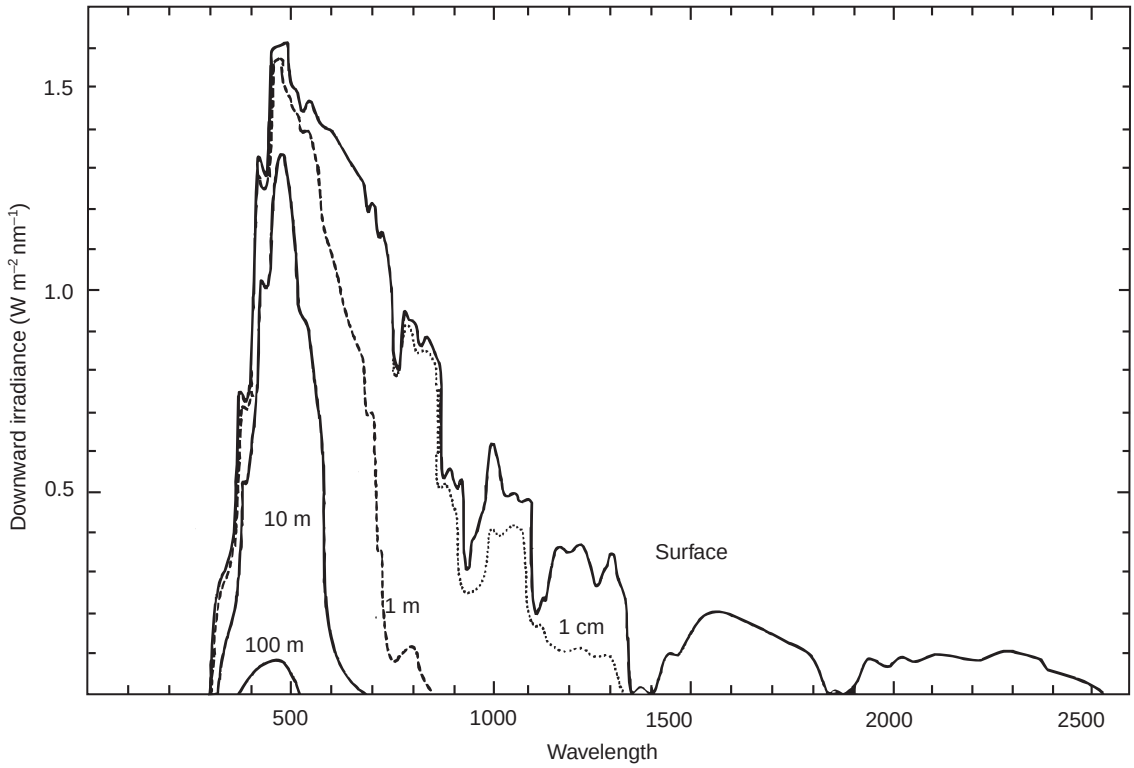

Figure 1 The spectrum of downward irradiance $E_d(z, \lambda)$ in the sea at different depths. (Adapted with permission from Jerlov, 1976.)

wavelength. If K_d is independent of z, monochromatic irradiance decreases exponentially with depth, consistent with Beer's law. K_d increases five orders of magnitude as wavelength increases from 500 to 2000 nm (**Figure 2**), consistent with the strong dependence of absorption on wavelength shown in **Figure 1**. In the wavelength band centered around 500 nm, K_d varies by a factor of 10 between the least absorbent and most absorbent cases.

The order of magnitude variation in K_d at 500 nm among the three cases (**Figure 2**) has a dramatic effect on net irradiance (**Figure 3**) because the peak of the solar spectrum is near 500 nm (**Figure 1**). Net irradiance, E, is the difference between net (wavelength integrated) downward and net upward irradiance. The difference between downward and net irradiance is negligible for most purposes because upward irradiance is typically 3% of downward irradiance within the ocean. At depths where the net downward irradiance is $< 10\%$ of its surface value, the decay with z is approximately exponential because light at these depths is roughly monochromatic.

The three cases with different optical properties (**Figures 2** and **3**) can be characterized biologically as oligotrophic, mesotrophic, and eutrophic (ranging from least to most absorbent). Oligotrophic water has low biological production and low nutrients. Eutrophic water has high biological production and high nutrients and mesotrophic water is moderate in both respects. The oligotrophic case

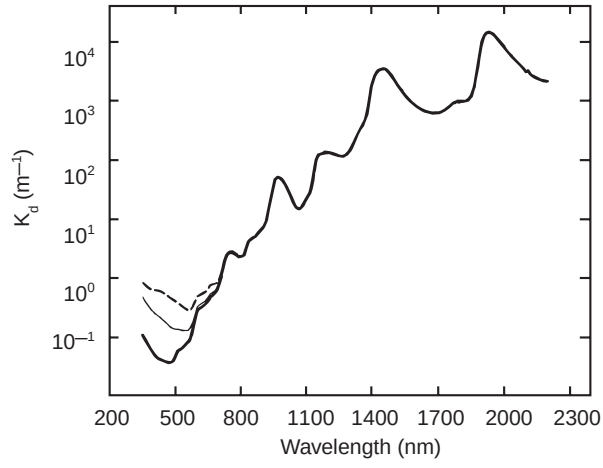

Figure 2 The diffuse attenuation coefficient for downward irradiance in sea water versus wavelength. Data for the wavelength band from 350 to 800 nm are from the Hydrolight radiative transfer model with the following conditions: depth 10 m, solar altitude 60°, cloudless sky, wind speed 2 m s^{-1}. The three lines (thin, thick, dashed) result from specified concentrations of chlorophyll (0.05, 1, 10 mg m^{-3}) and the beam attenuation coefficient at 440 nm for CDOM (0.01, 0.05, 0.1 m^{-1}). Data for the wavelength band from 800 to 2200 nm are for pure water. (Tabulations taken from Kuo *et al.*, 1993.)

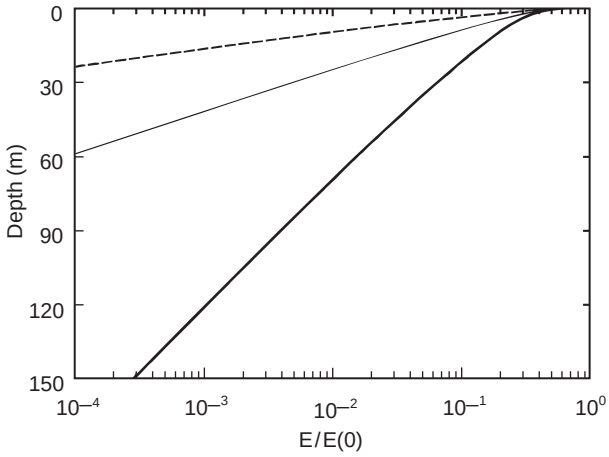

Figure 3 Net irradiance $E = (E_d - E_u)$ versus depth from the Hydrolight model for the conditions specified in the caption for **Figure 2**.

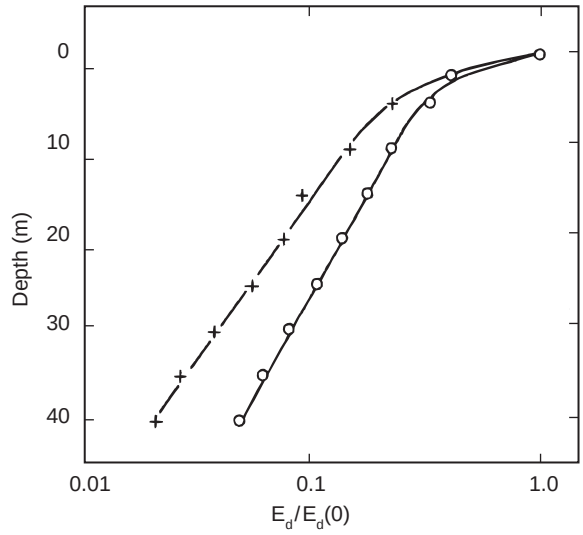

Figure 4 Measurements in the upper 40 m of downward irradiance normalized by downward irradiance just below the surface. The measurements were made in the North Pacific (35°N, 155°W) in February. The open circles are the average of five sets of observations with similar irradiance profiles; solar altitude ranged from 30° to 38° and the sky was overcast. The plus signs show one set of observations for which solar altitude was 16° and the sky was clear. The curves are the sum of two exponential terms fitted to the observations (see eqn [1]). (Adapted with permission from Paulson and Simpson, 1977.)

illustrated in **Figures 2** and **3** is typical of open-ocean water. Mesotrophic and eutrophic water are likely to be found near the coast.

Parameterized Irradiance versus Depth

Observations show that downward short-wave irradiance decreases exponentially with depth below a depth of about 10 m (**Figure 4**) as the result of absorption by the overlying sea water of all irradiance except for blue-green light. This suggests that E_d can be approximated by a sum of n exponential terms:

$$E_d/E_0 = \sum_{i=1}^{n} F_i \exp(K_i z) \qquad [1]$$

$$\sum_{i=1}^{n} F_i = 1$$

where F_i is the fraction of downward irradiance in a wavelength band i and K_i is the diffuse attenuation coefficient for the same band. The leading term in eqn [1] is defined as the short wavelength band that describes the exponential decay below 10 m (**Figure 4**). At least one additional term is required. A total of two terms fits the observations in **Figure 4** reasonably well, although accuracy in the upper few meters is lacking.

Jerlov has proposed a scheme for classifying oceanic waters according to their clarity. He defined five types (I, IA, IB, II, and III) ranging from the clearest open-ocean water (type I) to increasingly turbid water. Parameters for the sum of two exponential terms (eqn [1]) fit to the values of downward irradiance which define the Jerlov water types are given in **Table 2** and plots of values and fitted curves are shown in **Figure 5**. Apart from systematic disagreement in the upper few meters, the fit is good. Differences in the values of K_2 in **Table 2** are not significant. Water types IA and IB are not shown in **Figure 5**. However, the fits to the observations shown in **Figure 4** yield parameters very similar to those for types IA and IB (open circles and plus signs, respectively, in **Figure 4**). Most open-ocean water is intermediate between types I and II.

Table 2 Values of parameters determined by fitting the sum of two exponential terms (see eqn [1]) to values of downward irradiance which define Jerlov's (1976) water types

Water type	F_1	K_1 (m^{-1})	K_2 (m^{-1})	C ($mg\,m^{-1}$)
I	0.32	0.036	0.8	0–0.01
IA	0.38	0.049	1.7	~ 0.05
IB	0.33	0.058	1.0	~ 0.1
II	0.23	0.069	0.7	~ 0.5
III	0.22	0.13	0.7	~ 1.5–2.0

Values of downward irradiance in the upper 100 m were used, except that values were limited to the upper 50 m for type I because of a change in slope below 50 m. F_2 is $1 - F_1$. (Adapted from Paulson and Simpson, 1977.) The column labeled C is the approximate chlorophyll concentration for each water type as determined by Morel (1988).

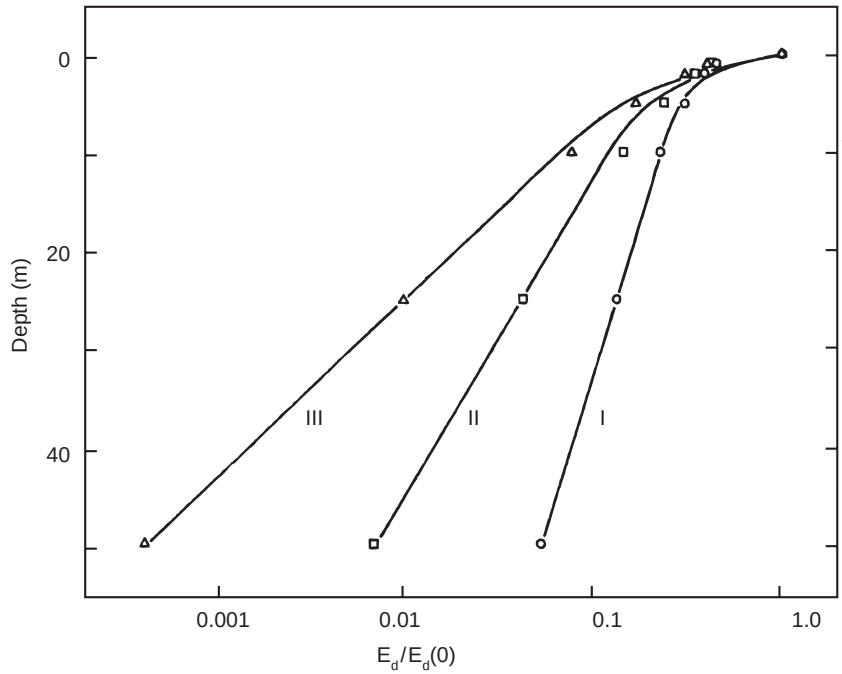

Figure 5 Normalized downward irradiance versus depth for water types I, II, and III. The data (open circles, squares, and triangles) are from Jerlov (1976) and the curves are a fit to the data with the parameters given in **Table 2**. (Adapted with permission from Paulson and Simpson, 1977.)

The approximate chlorophyll concentration for each of the Jerlov water types is given in **Table 2**.

The Jerlov water types can be compared to the oligotrophic, mesotrophic, and eutrophic cases illustrated in **Figures 2** and **3**. The oligotrophic case is intermediate between types IA and IB. The mesotrophic case is similar to type III and the eutrophic case is similar to Jerlov's coastal type 5 water.

The sum of two exponential terms (eqn [1]) is adequate for modeling purposes when the required vertical resolution is a few meters or greater. For a vertical resolution of 1 m or less, additional terms are required. These additional terms can be constructed with knowledge of the surface irradiance spectrum (**Figure 1**) and the diffuse attenuation coefficient versus wavelength (**Figure 2**).

See also

Bio-optical Models. Coastal Circulation Models. General Circulation Models. Heat and Momentum Fluxes at the Sea Surface. Inherent Optical Properties and Irradiance. Ocean Colour from Satellites. Photochemical Processes. Radiative Transfer in the Ocean. Upper Ocean Heat and Freshwater Budgets. Upper Ocean Time and Space Variability. Wind and Buoyancy-forced Upper Ocean.

Further Reading

Dera J (1992) *Marine Physics*. Amsterdam: Elsevier.

Jerlov NG (1976) *Marine Optics*. Amsterdam: Elsevier.

Kou L, Labrie D and Chylek P (1993) Refractive indices of water and ice in the 0.65- to 2.5-μm spectral range. *Applied Optics* 32: 3531–3540.

Kraus EB and Businger JA (1994) *Atmosphere–Ocean Interaction*, 2nd edn. New York: Oxford University Press.

Mobley CD (1994) *Light and Water*. San Diego: Academic Press.

Mobley CD and Sundman LK (2000) *Hydrolight 4.1 User's Guide*. Redmond, WA: Sequoia Scientific.

Monahan EC and O'Muircheartaigh IG (1987) Comments on glitter patterns of a wind-roughened sea surface. *Journal of Physical Oceanography* 17: 549–550.

Morel A (1988) Optical modeling of the upper ocean in relation to its biogenous matter content. *Journal of Geophysical Research* 93: 10749–10768.

Paulson CA and Simpson JJ (1977) Irradiance measurements in the upper ocean. *Journal of Physical Oceanography* 7: 952–956.

Payne RE (1972) Albedo of the sea surface. *Journal of Atmospheric Sciences* 29: 959–970.

Thomas GE and Stamnes K (1999) *Radiative Transfer in the Atmosphere and Ocean*. Cambridge: Cambridge University Press.

Tyler JE and Smith RC (1970) *Measurements of Spectral Irradiance Underwater*. New York: Gordon and Breach.